

# EVALUATION OF STRESS FIELD AT THE VERTEX OF THE INTERFACE IN THREE-DIMENSIONAL DISSIMILAR MATERIAL JOINTS

<sup>1</sup>SHAHIDUL ISLAM, <sup>2</sup>MINHAZ MORSHED, <sup>3</sup>A. H. M. ABDULLAH AL MAMUN

Department of Mechanical Engineering  
Khulna University of Engineering & Technology (KUET), Khulna-9203, BANGLADESH  
E-mail: <sup>1</sup>shahidulbitk@gmail.com, <sup>2</sup>mmpial@gmail.com, <sup>3</sup>mamoon2k6@gmail.com

---

**Abstract** - Dissimilar material joint has been used in many industrial products such as automobiles, smart material, medical equipment and electrical instruments. A mismatch of material properties and the coefficient of thermal expansion cause the failure of joints. The durability and performance of joints are affected by several parameters such as material property, external and internal forces. Hence, dissimilar material joints should be analyzed considering the properties of materials. Many investigators investigated firstly stress fields in 2D elastic dissimilar material joints and then those in 2D elasto-plastic dissimilar material joints. Recently, the 2D numerical analysis has been extended to 3D numerical analysis for determining the stress fields in elastic dissimilar material joints. However, the 3D stress field near the vertex of dissimilar material joints has not been clear until now. In the present paper, the effect of stress fields is evaluated using eigen value analysis based on a finite element method. In this analysis a model of three-dimensional dissimilar joint consisting of aluminum and resin is used. All stress components are expressed as spherical coordinate systems in which origins are located at the vertex of the interface. From numerical result, evaluation of the stress field is performed.

---

**Index Terms** - 3D stress field, dissimilar material, eigen analysis, FEM, smart material.

---

## I. INTRODUCTION

When dissimilar materials are jointed together, the stress singularity occurs near the free edges of the interface due to a mismatch of mechanical properties and thermal expansion coefficients of the joint components. The stress concentrations caused by mechanical or thermal loads may lead to crack initiation and extension, and sometimes the stress concentrations may be high enough to debond the material parts. Reliable service lifetime predictions of bonded components demand a complete understanding of the debonding processes of these materials. The stress fields are one of the main factors responsible for debonding under mechanical or thermal loading [1]. Over sixty years ago, many authors have determined the characteristics of singular stress fields at singular points in two-dimensional numerical analysis for elastic dissimilar material joints. Recently, some researchers have extended the two-dimensional numerical analysis to three-dimensional numerical analysis for elastic dissimilar material joints using the numerical methods that has the small number of element. By the way, the three-dimensional numerical analysis is still difficult to analyze in dissimilar material joints.

The study on this field has been carried out step by step. William used the numerical analysis for analyzing stress singularities in infinite wedges and applied to the analysis of stress distribution at the vicinity of a crack tip [2]. Aksentian determined eigen values and eigen vectors at a singular point in plane intersecting a free edge of the interface in three-dimensional dissimilar joints [3]. Kawai,

Fujitani and Kobayashi performed the stress analysis at a conical surface pit and applied Williams' method to a three-dimensional crack problem. Numerical analysis of characteristic roots for conical pit problem was analyzed for determining eigen values at the vertex of conical pit [4].

Yamada and Okumura developed a finite element analysis for solving eigen value equation to determine directly the order of stress singularity and the angular variation of the stress and displacement fields. This eigen analysis was used to evaluate the order of singularity at a point where a crack meets a free surface in an isotropic material [5]. Then, Pageau, Joseph and Biggers adapted the eigen analysis based on a finite element for analyzing the inplane deformation of wedges and junctions that composed of anisotropic materials. The stress and displacement fields were obtained from eigen formulation for real and complex orders of stress singularity [6].

Koguchi examined the order of stress singularity at a vertex and also along the stress singularity line between two isotropic materials in joints using eigen analysis. The stress distributions around the vertex were determined using a boundary element method (BEM) [7]. Koguchi determined the intensity of singularity by fitting the stress profile that obtained from BEM analysis with a least square method [8]. Dimitov, Andra and Schnake presented the three-dimensional eigen analysis that used Arnoldi method. This method needs only the small-banded matrix when compared with normally used determinant method. The order of singularities at corners and free edges of the interface in laminate

composite material joints were determined using the eigen analysis [9].

Lee and Im used a two-state M-integral for computing the near-tip stress intensities around three-dimensional wedges and used an eigen analysis for determining eigen values and eigen vectors [10]. Apel, Leguillon, Pester and Yosibash determined edge singularity by the use of three-dimensional Williams' expansion. The edge stress intensity factors along the reentrant wedge front were determined using a quasi-dual function method [11]. Yosibash, Omer and Dauge computed the complex eigen function by using a p-version finite element method and examined the edge stress intensity factors at the edge vicinity in three-dimensional anisotropic multi-material interfaces using a quasi-dual function method [12]. T. Ikeda, H. Hirai, and M. Abe, proposed the solution of singular stress field and its SIFs of an interfacial corner of a 2D dissimilar piezoelectric material joints using extended Stroh formalism [13]. So, several studies have investigated the stress field in 3D elastic materials. Recently, some researcher proposed the solution of singular stress field and its stress intensity factors of an interfacial corner of a 2D dissimilar anisotropic material joint with crack. However, the stress field at a vertex in 3D dissimilar bonded joints has not been made clear until now. In this paper, the stress field at a vertex of interface is investigated in dissimilar joints.

## II. THE BASIC EQUATION

The FEM formulation can be expressed from the total of potential energy at equilibrium condition. The total of potential energy  $J^*$  is in the form of the following equation.

$$J^* = U^* + W^* \quad (1)$$

Where  $U^*$  is the internal strain energy. For the linear elastic material, the internal strain energy of the system that has a volume (V) is given by

$$U^* = \frac{1}{2} \int_V [\varepsilon]^T [C] [\varepsilon] dV \quad (2)$$

Where  $[\varepsilon]$  is strain matrix and  $[C]$  is elasticity matrix of modulus  $W^*$  is the potential energy due to external forces such as body force (F) on a volume (V) and surface traction on a surface (S). The potential energy due to external forces is simply given by and it will be

$$W^* = - \int_V (F_x u + F_y v + F_z w) dV - \int_S (T_x u + T_y v + T_z w) dS \quad (3)$$

and it will be

$$W^* = - \int_V [U]^T \{F\} dV - \int_S [U]^T \{T\} dS. \quad (4)$$

Where the vector  $[U]$  is the virtual displacements (u, v, w) in directions (x, y, z) of the Cartesian coordinate. Here the total of potential energy is obtained by substituting (2) and (4) into (1). It becomes as the following equation.

$$J^* = \frac{1}{2} \int_V [\varepsilon]^T [C] [\varepsilon] dV - \int_V [U]^T \{F\} dV - \int_S [U]^T \{T\} dS \quad (5)$$

The displacement formulation for an e nodes element is expressed as the following equation.

$$u_i = \sum_{n=1}^e N_n \bar{u}_{in} \quad (6)$$

Where  $u_i$  is the displacement in direction i.  $\bar{u}_{in}$  is the displacement at node n associated with direction i.  $N_n$  is the interpolation function at node n.

Using the equation above, the vector of strain in (5) can be expressed with the form of displacement as follows:

$$\{\varepsilon\} = \begin{Bmatrix} \varepsilon_x \\ \varepsilon_y \\ \varepsilon_z \\ \gamma_{xy} \\ \gamma_{yz} \end{Bmatrix} = \begin{Bmatrix} \frac{\partial u}{\partial x} \\ \frac{\partial v}{\partial y} \\ \frac{\partial w}{\partial z} \\ \frac{\partial u}{\partial y} + \frac{\partial v}{\partial x} \\ \frac{\partial u}{\partial z} + \frac{\partial w}{\partial x} \\ \frac{\partial v}{\partial z} + \frac{\partial w}{\partial y} \end{Bmatrix} = [B] \{\bar{U}\} \quad (7)$$

Where  $[B]$  is the differential operator matrix in the form of the differential of interpolation functions. The total of potential energy equation becomes

$$J^* = \frac{1}{2} \int_V \{\bar{U}\}^T [B]^T [C] [B] \{\bar{U}\} dV - \int_V \{\bar{U}\}^T [N]^T \{F\} dV - \int_S \{\bar{U}\}^T [N]^T \{T\} dS \quad (8)$$

The total of potential energy is minimum when it is being in the equilibrium condition. The variation of the total of potential energy ( $\delta J^*$ ) in this state must be stationary for variation of the displacement. It means that the variation of the total of potential energy becomes zero as equation below:

$$\delta J^* = \frac{\partial J^*}{\partial \bar{U}} = \frac{\partial (U^* + W^*)}{\partial \bar{U}} = 0 \quad (9)$$

The finite element equation of the total of potential energy is expressed as

$$J^* = \frac{1}{2} \{\bar{U}\}^T [K^*] \{\bar{U}\} - \{\bar{U}\}^T \{F_B\} - \{\bar{U}\}^T \{F_t\} \quad (10)$$

$$\frac{\partial J^*}{\partial \bar{U}} = [K^*] \{\bar{U}\} + \{F_B\} + \{F_t\} = 0$$

and it is simply given by

$$[K^*] \{\bar{U}\} = \{F_B\} + \{F_t\}. \quad (11)$$

Where

$$[K^*] = \int_V [B]^T [C] [B] dV \quad (12)$$

$$\{F_B\} = \int_V [N]^T \{F\} dV \quad (13)$$

$$\{F_t\} = \int_S [N]^T \{T\} dS \quad (14)$$

$[K^*]$  is the stiffness matrix and  $\{F_B\}, \{F_t\}$  are the load

vectors form body forces and traction forces, respectively.

The displacement values at each node in directions x, y and z are solving from the finite element equation as given in (11). The hexahedron element can be considered as Fig. 1. The interpolation functions at each node is given by

$$N_n = \frac{1}{8}(1 + \xi_n \xi)(1 + \eta_n \eta)(1 + \zeta_n \zeta) \quad (15)$$

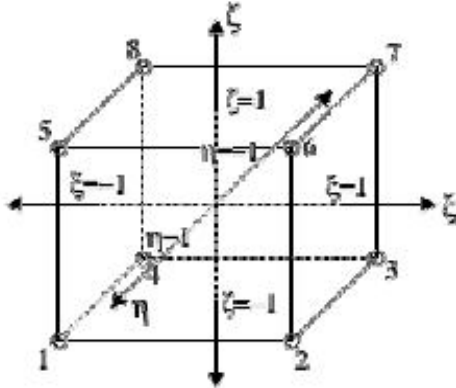


Fig. 1 Hexahedron element and its local geometry

The matrix [C] for a hexahedron element is

$$[C] = \frac{E}{(1+\nu)(1-2\nu)} \begin{bmatrix} (1-\nu) & \nu & \nu & 0 & 0 & 0 \\ & (1-\nu) & \nu & 0 & 0 & 0 \\ & & (1-\nu) & 0 & 0 & 0 \\ & & & \frac{(1-2\nu)}{2} & 0 & 0 \\ & & & & \frac{(1-2\nu)}{2} & 0 \\ & & & & & \frac{(1-2\nu)}{2} \\ SYM & & & & & \end{bmatrix} \quad (16)$$

where E is Young's Modulus and n is Poisson's ratio.

The stiffness matrix  $[K^*]$  can be calculated by using

Gauss-Legendre integration formula. Thus the  $[K^*]$  matrix in (12) becomes

$$[K^*] = \int_{-1}^1 \int_{-1}^1 \int_{-1}^1 [B(\xi, \eta, \zeta)]^T [C] [B(\xi, \eta, \zeta)] |J|(\xi, \eta, \zeta) d\xi d\eta d\zeta \quad (17)$$

$$\approx \sum_{i=1}^{NG} \sum_{j=1}^{NG} \sum_{k=1}^{NG} W_i W_j W_k [B(\xi_i, \eta_j, \zeta_k)]^T [C] [B(\xi_i, \eta_j, \zeta_k)] |J|(\xi_i, \eta_j, \zeta_k) d\xi d\eta d\zeta$$

Where  $|J|$  is the determinant of the Jacobian transformation between the global and local volume coordinates. W is the weight with the subscripts (i, j, k) and NG is the number of Gauss points. For the plane (x, y) problem, the stiffness matrix becomes

$$[K^*] = \int_{\Omega} [B]^T [C] [B] dS \quad (18)$$

$$\{F_B\} = \int_{\Omega} [N]^T \{F\} dS \quad (19)$$

$$\{F_i\} = \int_{x_a} [N]^T \{T_x\} dx \quad \text{or} \quad \int_{y_b} [N]^T \{T_y\} dy \quad (20)$$

The matrix [C] for plane stress case is

$$[C] = \frac{E}{1-\nu^2} \begin{bmatrix} 1 & \nu & 0 \\ & 1 & 0 \\ SYM & & \frac{1-\nu}{2} \end{bmatrix} \quad (21)$$

The matrix [C] for plane strain case is

$$[C] = \frac{E}{1+\nu} \begin{bmatrix} \frac{1-\nu}{1-2\nu} & \frac{\nu}{1-2\nu} & 0 \\ & \frac{1-\nu}{1-2\nu} & 0 \\ SYM & & \frac{1}{2} \end{bmatrix} \quad (22)$$

Finally, stress component is in the form of the following equation

$$\{\sigma\} = [C] \{\varepsilon\} \quad (23)$$

The stiffness matrix  $[K^*]$  in (18) can be also

calculated as the same as three-dimensional FEM by using Gauss-Legendre integration formula.

$$[K^*] = \int_{-1}^1 \int_{-1}^1 [B(\xi, \eta)]^T [C] [B(\xi, \eta)] |J|(\xi, \eta) d\xi d\eta$$

$$\approx \sum_{i=1}^{NG} \sum_{j=1}^{NG} W_i W_j [B(\xi_i, \eta_j)]^T [C] [B(\xi_i, \eta_j)] |J|(\xi_i, \eta_j) d\xi d\eta \quad (24)$$

### III. THREE-DIMENSIONAL EIGEN ANALYSIS USING FEM

Fig. 2 shows the definition of the finite element geometry and natural coordinates at a free-edge singular point on a spherical domain of a typical case where a singular stress state occurs at point S. The spherical domain surrounding the singular point S is divided into a number of 8-node quadrilateral elements that are located in spherical coordina  $(r, \theta, \phi)$ . The natural coordinates  $(\xi^*, \eta^*, \zeta^*)$  in each element have those ranges between 1 and -1.

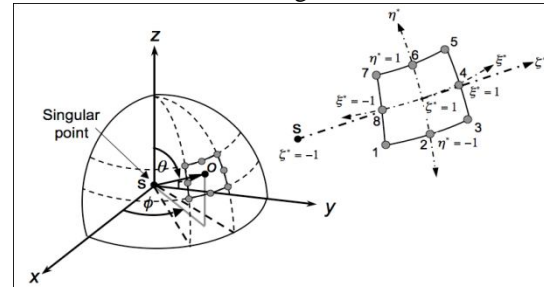


Fig. 2 Definition of the finite element geometry and natural coordinates at a free-edge singular point on a spherical domain



A point O is located by the singular transformation of Yamada [5] as the following equation.

$$r - \rho r_0 - r_0 \left( \frac{1 + \xi^*}{2} \right)^{\frac{1}{p}}, \quad 0 = \sum_{n=1}^8 H_n \theta_n \quad \text{and} \quad \phi = \sum_{n=1}^8 H_n \phi_n \quad (25)$$

The interpolation functions of the 8-nodes quadrilateral element at nodes n are expressed as the following equations.

When n is located at the corner nodes in the element,

$$H_n = \frac{1}{4} (1 + \xi_n^* \xi^*) (1 + \eta_n^* \eta^*) (\xi_n^* \xi^* + \eta_n^* \eta^* - 1) \quad (26)$$

When n is located at the middle nodes which  $\xi_n^*$  is zero in the element,

$$H_n = \frac{1}{2} (1 - \xi^{*2}) (1 + \eta_n^* \eta^*) \quad (27)$$

When n is located at the middle nodes which  $\eta_n^*$  is zero in the element,

$$H_n = \frac{1}{2} (1 + \xi_n^* \xi^*) (1 - \eta^*) \quad (28)$$

The displacement at the singular point is taken as zero and the displacement fields around the singular point in i-directions are assumed to be

$$\{u_i^*\} = \left( \frac{r}{r_0} \right)^p \left[ \sum_{n=1}^8 H_n \bar{u}_{in}^* \right] \quad (29)$$

The Jacobian matrix for transferring the spherical coordinates to the natural coordinates is

$$[J] = \begin{bmatrix} \frac{\partial r}{\partial \xi^*} & \frac{\partial \theta}{\partial \xi^*} & \frac{\partial \phi}{\partial \xi^*} \\ \frac{\partial r}{\partial \eta^*} & \frac{\partial \theta}{\partial \eta^*} & \frac{\partial \phi}{\partial \eta^*} \\ \frac{\partial r}{\partial \xi^*} & \frac{\partial \theta}{\partial \xi^*} & \frac{\partial \phi}{\partial \xi^*} \end{bmatrix} = \begin{bmatrix} 0 & \sum_{n=1}^8 H_{n,\xi^*} \theta_n & \sum_{n=1}^8 H_{n,\xi^*} \phi_n \\ 0 & \sum_{n=1}^8 H_{n,\eta^*} \theta_n & \sum_{n=1}^8 H_{n,\eta^*} \phi_n \\ \frac{r_0}{2p} \rho^{1-p} & 0 & 0 \end{bmatrix} \quad (30)$$

In each element, it is no relationship between the radius coordinate and the angular coordinates. Thus the Jacobian matrix can be preferable in the form of equation below:

$$[J] = \begin{bmatrix} \sum_{n=1}^8 H_{n,\xi^*} \theta_n & \sum_{n=1}^8 H_{n,\xi^*} \phi_n \\ \sum_{n=1}^8 H_{n,\eta^*} \theta_n & \sum_{n=1}^8 H_{n,\eta^*} \phi_n \end{bmatrix} \quad (31)$$

Then the strain matrix is

$$\{\varepsilon\} = \begin{Bmatrix} \varepsilon_r \\ \varepsilon_\theta \\ \varepsilon_\phi \\ \gamma_{r\theta} \\ \gamma_{r\phi} \\ \gamma_{\theta\phi} \end{Bmatrix} = \sum_{n=1}^8 [B_n] \{u_n^*\} = [B] \{u_i^*\}, \quad \{u_n^*\} = \begin{Bmatrix} \bar{u}_{rn}^* \\ \bar{u}_{\theta n}^* \\ \bar{u}_{\phi n}^* \end{Bmatrix} \quad (32)$$

Where

$$[B] = \frac{1}{r_0} \rho^{p-1} (\nu [B_s] + [B_b]), \quad [B_m] = \begin{bmatrix} H_n & 0 & 0 \\ 0 & 0 & 0 \\ 0 & 0 & 0 \\ 0 & H_n & 0 \\ 0 & 0 & H_n \\ 0 & 0 & 0 \end{bmatrix} \quad (33)$$

$$[B_{bn}] = \begin{bmatrix} 0 & 0 & 0 \\ H_n & A_1 & 0 \\ H_n & H_n \cot(\theta) & A_2 \\ A_1 & -H_n & 0 \\ A_2 & 0 & -H_n \\ 0 & A_2 & A_1 - H_n \cot(\theta) \end{bmatrix} \quad (33)$$

$$A_1 = [J(1,1)]^{-1} \left[ \frac{\partial H_n}{\partial \xi^*} \right] + [J(1,2)]^{-1} \left[ \frac{\partial H_n}{\partial \eta^*} \right]$$

$$A_2 = \frac{[J(2,1)]^{-1} \left[ \frac{\partial H_n}{\partial \xi^*} \right] + [J(2,2)]^{-1} \left[ \frac{\partial H_n}{\partial \eta^*} \right]}{\sin(\theta)} \quad (34)$$

Using the finite element method, the formula should be firstly considered in the equilibrium of the principle of virtual work. It is given by

$$\int_{r_0}^r \int_{\theta}^{\theta} \int_{\phi}^{\phi} \left( \sigma_{rr} \delta \varepsilon_{rr} + \sigma_{\theta\theta} \delta \varepsilon_{\theta\theta} + \sigma_{\phi\phi} \delta \varepsilon_{\phi\phi} + \sigma_{r\theta} \delta \varepsilon_{r\theta} + \sigma_{r\phi} \delta \varepsilon_{r\phi} + \sigma_{\theta\phi} \delta \varepsilon_{\theta\phi} \right) r^2 \sin(\theta) dr d\theta d\phi = \left( I_{rr} \delta u_{r0} + I_{r\theta} \delta u_{\theta 0} + I_{r\phi} \delta u_{\phi 0} \right) \sin(\theta) d\theta d\phi \quad (35)$$

Where  $u_{r0}^*$ ,  $u_{\theta 0}^*$  and  $u_{\phi 0}^*$  are the displacement on the surface  $r = r_0$ . Then using (25) to (30), the equation (35) becomes

$$\int_{-1}^1 \int_{-1}^1 \int_{-1}^1 r_0^2 \rho^2 \left( \delta \{\varepsilon\}^T \{\sigma\} \right) \sin(\theta) |J| d\xi^* d\eta^* d\theta = \int_{-1}^1 \int_{-1}^1 r_0^2 \left( \delta \{u_o^*\}^T \{T\} \right) \sin(\theta) |J_1| d\xi^* d\eta^* \quad (36)$$

where the determinant  $|J_1| = 2p / (r_0 \rho^{p-1}) |J|$ .

In the view of (33) and (35), the finite element formulation for solving the root p, is expressed using the relation  $\{\sigma\} = [C] \{\varepsilon\}$  as

$$\delta \{u_o^*\}^T \int_{-1}^1 \int_{-1}^1 \left( p [B_{an}]^T + [B_{bn}]^T \right) [C] (p [B_{an}] + [B_{bn}]) \sin(\theta) |J_1| d\xi^* d\eta^* \{u_o^*\} = \delta \{u_o^*\}^T \int_{-1}^1 \int_{-1}^1 [H]^T [C] (p [B_{an}] + [B_{bn}]) \sin(\theta) |J_1| d\xi^* d\eta^* \{u_o^*\} \quad (37)$$

Then it can be simply given in the form of

$$\left( p^2 [\bar{A}] + p [\bar{B}] + [\bar{C}] \right) \{U\} = 0 \quad (38)$$

Where

$$[\bar{A}] = \sum_{\xi} ([k_{\alpha}^*] [k_{\xi\alpha}^*]), \quad [\bar{B}] = \sum_{\xi} ([k_{\beta}^*] [k_{\xi\beta}^*])$$

$$[\bar{C}] = \sum_{\xi} ([k_{\gamma}^*]), \quad \{U\} = \sum_{\xi} \{U\}$$

The summation over  $\xi$  means the assembly of all elements into the global model. The matrix [C] represents an elastic moduli matrix 6 × 6 and [C] is comprised of the first, fourth and fifth rows of matrix [C].

#### IV. PROBLEM DESCRIPTION AND MODEL OF ANALYSIS

Figure 3 represents a model for 3D dissimilar material joint used in the present analysis. The dimensions of the model is 10×10×20 mm. Aluminum and Resin are used for Materials 1 and 2, respectively, in the analysis. Fig. 3 represents the geometry of a typical case where a singular stress occurs at the point o. The region surrounding the singular point is divided into a number of quadratic elements with a summit o, with each element being located in spherical coordinates r,  $\theta$ , and  $\phi$  by its nodes 1 to 8. Fig. 4 represents a mesh model on the developed  $\phi$ - $\theta$  plane.

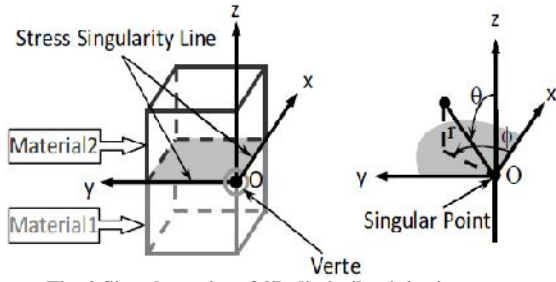


Fig. 3 Singular point of 3D dissimilar joint in x-, y-, z-coordinates

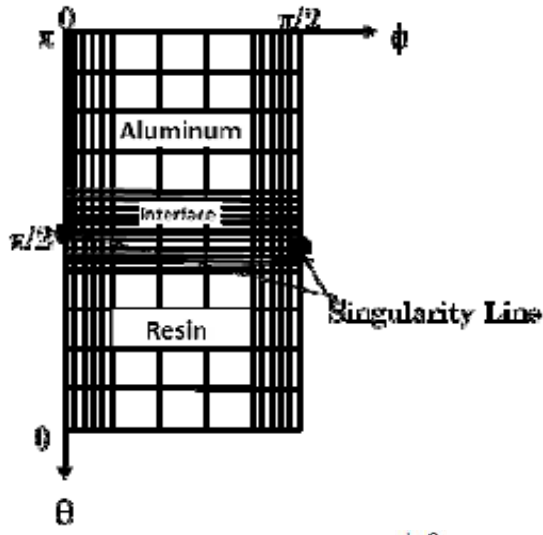


Fig. 4 A mesh model on the developed  $\phi$ - $\theta$  plane

Material	Young's modulus, E (GPa)	Poisson's ratio, $\nu$
Resin	2.74	0.38
Aluminum	69	0.32

Table 1 Material property of Resin and Aluminum

## V. NUMERICAL RESULT AND DISCUSSION

Angular functions obtained from eigen equation, (38), are examined [14]. Distributions of angular function of elastic displacement and electric potential on a  $\theta$ - $\phi$  plane are shown in Fig. 5 and distributions of angular function of stress and electric displacement are in shown in Figs. 6~ 8. Solving eigen equation yields many roots  $p$  and eigen vectors corresponding to each eigen value are obtained. However, if the root  $p$  is within the range of  $0 < p < 1$ , this fact indicates that the stress field has singularity. The eigen value and the order of singularity at the singularity corner is  $p = 0.6395$  and  $\lambda = 0.3605$  and at the singularity line is  $p = 0.7204$  and  $\lambda = 0.2796$ .

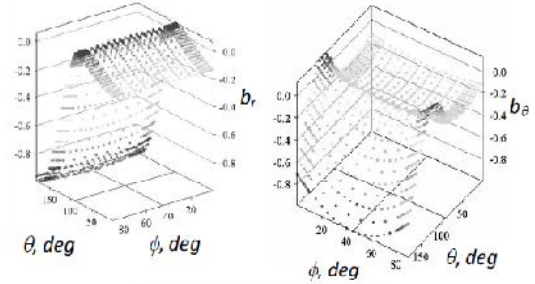


Fig. 5 Distribution of  $b_i$  against  $\phi$  &  $\theta$  for Resin & Aluminum

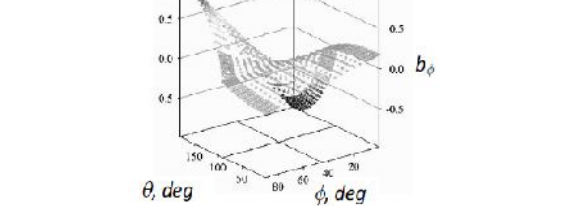


Fig. 6 Distribution of  $f_{r\theta}$  against  $\phi$  &  $\theta$  for Resin & Aluminum

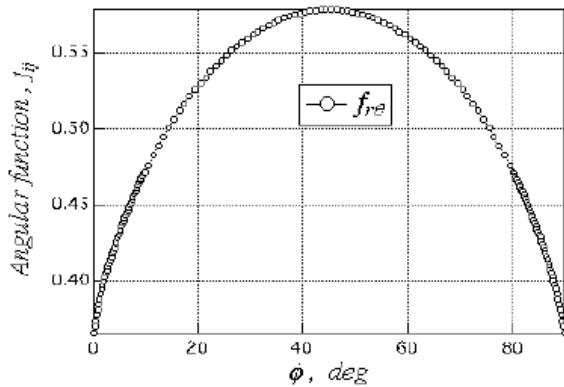


Fig. 7 Distribution of  $f_{\theta\theta}$  against  $\phi$  &  $\theta$  for Resin & Aluminum

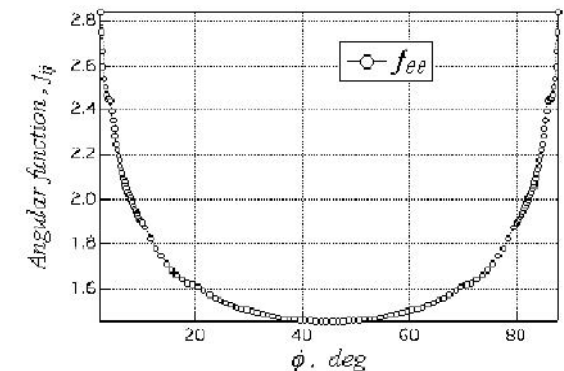


Fig. 8 Distribution of  $f_{\theta\phi}$  against  $\phi$  &  $\theta$  for Resin & Aluminum

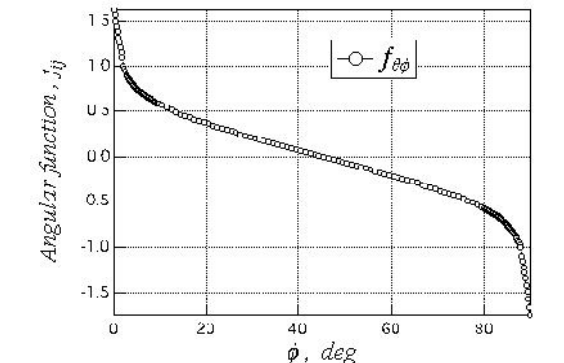


Fig. 9 Distribution of  $f_{\phi\phi}$  against  $\phi$  &  $\theta$  for Resin & Aluminum

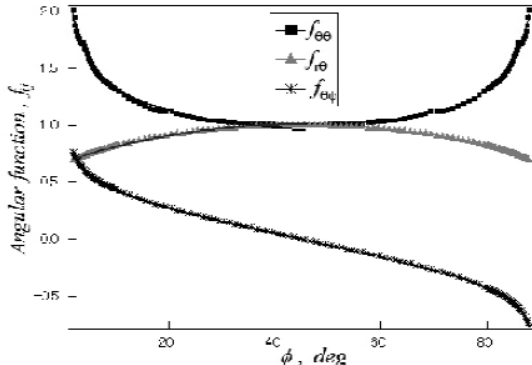
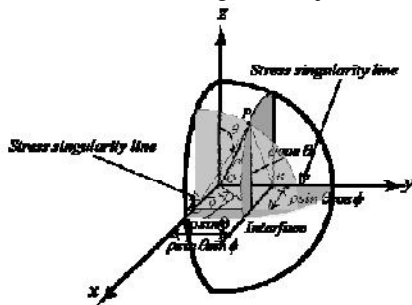


Fig.9 Distribution of normalized  $f_{ij}$  against  $\phi$  at  $\theta = 90^\circ$  for Resin & Aluminum

The normalized angular function of stress is shown in Fig.9 for  $\lambda = 0.3605$ . The angular function of stress against the angle  $\phi$  at  $\theta = 90^\circ$  is plotted. The stress singularity lines are at the free edge of the material joint. The graph shows that the value of stress increases rapidly near the interface edge than the inner portion of the joints. The value of  $f_{r,\theta}$  and  $f_{\theta\theta}$  is one and  $f_{\phi\theta}$  is zero near  $\phi = 45^\circ$ . After that the values of angular function of stress are increased. Near interface edge of the joint has the largest value of angular function. So there is a possibility of debonding and delamination occur near the interface edge of the joint.



The coefficient of angular function of stress for one side is expressed by the following equation.

$$f_{\theta\theta}^A(\phi) = I_{1\theta\theta}^A (\sin \phi)^{-\lambda_{1\theta\theta}^A} + I_{2\theta\theta}^A + \sum_{k=3}^n I_{k\theta\theta}^A \{\ln(\sin \phi)\}^{k-2} \quad (39)$$

$$f_{r\theta}^A(\phi) = I_{1r\theta}^A \cos \phi (\sin \phi)^{-\lambda_{1r\theta}^A} + I_{2r\theta}^A (\sin \phi)^{-\lambda_{2r\theta}^A} + I_{3r\theta}^A (\cos \phi \sin \phi) \left[ \sum_{k=4}^{n+1} I_{kr\theta}^A \left[ \cos \phi \{\ln(\sin \phi)\}^{k-2} + \sin \phi \{\ln(\sin \phi)\}^{k-2} \right] \right] \quad (40)$$

$$f_{\phi\theta}^A(\phi) = I_{1\phi\theta}^A \cos \phi (\sin \phi)^{-\lambda_{1\phi\theta}^A} + I_{2\phi\theta}^A (\sin \phi)^{1-\lambda_{2\phi\theta}^A} + I_{3\phi\theta}^A (\cos \phi - \sin \phi) \left[ \sum_{k=4}^{n+1} I_{k\phi\theta}^A \left[ \cos \phi \{\ln(\sin \phi)\}^{k-2} - \sin \phi \{\ln(\sin \phi)\}^{k-2} \right] \right] \quad (41)$$

Where  $f_{ij}$  and  $L_{ij}$  represent the angular function of stress and coefficient of angular function respectively. Furthermore, logarithmic terms in the above expressions are neglected, and then the coefficient of angular function for one side is determined by the following equations [14].

$$f_{\theta\theta}^A(\phi) = L_{1\theta\theta}^A (\sin \phi)^{-\lambda_{1\theta\theta}^A} + L_{2\theta\theta}^A \quad (42)$$

$$f_{r\theta}^A(\phi) = L_{1r\theta}^A \cos \phi (\sin \phi)^{-\lambda_{1r\theta}^A} + L_{2r\theta}^A (\sin \phi)^{1-\lambda_{2r\theta}^A} \quad (43)$$

$$f_{\phi\theta}^A(\phi) = L_{1\phi\theta}^A \cos \phi (\sin \phi)^{-\lambda_{1\phi\theta}^A} + L_{2\phi\theta}^A (\sin \phi)^{1-\lambda_{2\phi\theta}^A} \quad (44)$$

The coefficient of angular function is determined for line singularity,  $\lambda_1 = 0.2796$  by fitting the normalized

angular function of stress curve with the help of (42)~(44). The value of coefficient of angular function is shown in the Table 2. The value of  $L_1, N_1$  and  $L_2, N_2$  represent the power law term and second term respectively.

Material	Resin & Aluminum					
	$f_{\theta\theta}$		$f_{r\theta}$		$f_{\phi\theta}$	
Coefficient of angular function						
Power law term	$L_{1\theta\theta}$	0.916	$L_{1r\theta}$	-0.012	$L_{1\phi\theta}$	-0.256
2nd term	$L_{2\theta\theta}$	-0.098	$L_{2r\theta}$	-0.710	$L_{2\phi\theta}$	-0.248

Table 2 Coefficient of angular function (stress) for Resin & Aluminum

## CONCLUSION

An eigen equation formulation near the vertex of 3D dissimilar material joint was presented. Angular functions for singularity corner were derived from eigen analysis using a finite element method. From the numerical results, it is shown that the larger value of the angular function occurs at the interface edge in the material joint than the inner portion of the joint. It is suggested that delamination of the interface may occur at the interface edge of the piezoelectric material joints.

## REFERENCES

- [1] H. Koguchi, "Stress singularity analysis in three-dimensional bonded structure," Int. Journal of Solid Structures, Vol. 34, pp. 461-480, 1996.
- [2] M. L. Williams, "The Stress Around a Fault or Crack in Dissimilar Media", Bulletin of the Seismological Society of America, Vol. 49, pp. 199-204, April 1959.
- [3] O. K. Aksenian, "Singularities of the Stress-Strain State of A Plate in The Neighborhood of An Edge", PMM, Vol. 31, no. 1, pp.178-186, 1967.
- [4] T. Kawai, Y. Fujitani and M. Kobayashi, "Stress Analysis of the Conical Surface Pit Problem", Proc. Int. Conference of Fracture Mechanic and Technology, Hong Kong, Vol.2, pp. 1165-1170, March 1977.
- [5] Y. Yamada and H. Okumura, "Analysis of Local Stress in Composite Materials by the 3-D Finite Element", In Proc. Japan-U.S.A. Conference (Edited by K. Kawata and T. Akasaka), pp. 55-64, 1981.
- [6] S. S. Pageau, P. F. Joseph and Jr S. B. Biggers, "Finite Element Analysis of Anisotropic Materials with Singular Inplane Stress Fields", Int. Journal of Solid Structures, Vol. 32, pp. 571-591, 1995..
- [7] H. Koguchi, "Stress singularity analysis in three-dimensional bonded structure", Int. Journal of Solid Structures, Vol. 34, pp. 461-480 1996.
- [8] H. Koguchi, "Stress singularity analysis in three-dimensional bonded structure", Transactions of the JSME, Vol. 72, No. 724-A, pp. 2058-2065, 2006.
- [9] Dimitrov, H. Andra and E. Schnack, "Efficient computation of order and mode of corner singularities in 3D-elasticity", Int. Journal of Fracture, Vol. 115, pp. 361-375, 2002.
- [10] Y. Lee and S. Im, "On the computation of the near-tip stress intensities for three-dimensional wedges via two-state M-integral", Journal of Mechanics physics and Solids, Vol. 51, pp. 825-850, 2003.
- [11] T. Apel, D. Leguillon, C. Pester and Z. Yosibash, "Edge singularities and structure of the 3-D Williams

- expansion”, C R Mecanique, Vol. 336, pp. 629-635, 2008.
- [12] Z. Yosibash, N. Omer, and M. Dauge, “Edge stress intensity functions in 3-D anisotropic composites”, Composites Science and Technology, Vol. 68, pp. 1216-1224, 2008,.
- [13] T. Ikeda, H. Hirai, and M. Abe, “Stress intensity factor analysis of an interfacial corner between piezoelectric bimetals in a two-dimensional structure using H-integral Method,” Proceedings of the ASME, InterPACK, pp. 1-9, 2011.
- [14] M. S. Islam, and H. Koguchi, “Investigation of order of singularity in 3D transversely isotropic piezoelectric biomaterial joints by FEM,” Journal of Circuits, Systems, and Computer, vol. 24, pp. 1540001-21, 2015.

★ ★ ★